



Structural analysis of $\text{Ba}_{0.8}\text{Sr}_{0.2}\text{Ti}_{0.6}\text{Zr}_{0.3}\text{Mn}_{0.1}\text{O}_3$ ceramics

G. Murugesan ¹, Nandhan K. R. ^{2,a)}, N. Maruthi,² A. Muthuraja,³ Saraswathi Bhaskar,¹ and M. Manigandan^{1,4}

¹Department of Physics, Vel Tech Rangarajan Dr. Sagunthala R and D Institute of Science and Technology, Chennai 600062, Tamil Nadu, India

²Department of Physics, Faculty of Engineering and Technology, Jain University, Bangalore 562112, Karnataka, India

³Department of Physics, Theivanai Ammal College for Women (Autonomous), Villupuram, Tamil Nadu, India

⁴Department of Physics, Government Arts and Science College, Thiruvannainallur, Villupuram, Tamil Nadu, India

(Received 4 May 2022; accepted 30 November 2022)

Polycrystalline $\text{Ba}_{0.8}\text{Sr}_{0.2}\text{Ti}_{0.6}\text{Zr}_{0.3}\text{Mn}_{0.1}\text{O}_3$ was synthesized by solid-state reaction at 1600°C. The single phase formation of the compound without any impurities was confirmed by the X-ray diffraction technique. The prepared compound crystallized to a cubic structure with a space group of Pm-3m and the refined lattice parameters were $a = b = c = 4.0253 \text{ \AA}$, $\alpha = \beta = \gamma = 90^\circ$. Rietveld refinement was carried for the powder XRD data using GSAS software and the experimental data peaks were indexed by Powder X software.

© Jain (Deemed-to-be University), Bangalore, 2023. Published by Cambridge University Press on behalf of International Centre for Diffraction Data.

[doi:10.1017/S0885715622000598]

Key words: Rietveld refinement, oxides, X-ray diffraction

I. INTRODUCTION

Barium titanate ceramics have gained lot of attention in the scientific community due to the variation of properties due to the doping in barium or titanium sites (Levin et al., 2011). Due to its non-toxic behavior, BaTiO_3 is a better alternative to lead-based materials (Xue et al., 2011). BaTiO_3 possess superior ferroelectric behavior and has three phase transitions at different temperature regimes. At around -80°C , it transforms from rhombohedral to orthorhombic, at around 5°C , it transforms from orthorhombic to tetragonal, and at around 130°C , it transforms from tetragonal to cubic (Zhou et al., 1999). The temperature for phase transformation in BaTiO_3 shifts due to the A-site doping of Sr^{2+} or Ca^{2+} and B-site doping of Mn^{4+} , Fe^{2+} , Zr^{4+} , and Nb^{5+} making it suitable for high- or low-temperature piezoelectric device fabrication (Sindhu et al., 2013). The B-site substitution of Zirconium tunes the dielectric behavior of BaTiO_3 and increases its permittivity (Wang et al., 2014). The substitution of Mn and Zr in B-site leads to the formation of oxygen vacancy due to the charge imbalance and these oxygen vacancies induce magnetism in ceramics (Das et al., 2012).

The variation of Strontium content in BaTiO_3 shifts the transition and alters the electrical properties. Earlier reports have suggested that the doping of strontium in barium site leads to a transformation in the crystal structure from tetragonal to cubic (Sindhu et al., 2013). The smaller ionic radii of Sr^{2+} (1.44 Å) in comparison with Ba^{2+} (1.61 Å) has led to the reduction of c/a ratio and shifting of tetragonal structure to ideal cubic structure (Yu et al., 2015). In our sample, we also experienced the transformation of crystal structure from

tetragonal to cubic due to the increasing strontium concentration. The crystal structure for $\text{Ba}_{1-x}\text{Sr}_x\text{Ti}_{0.6}\text{Zr}_{0.3}\text{Mn}_{0.1}\text{O}_3$ exhibited a tetragonal structure for $x = 0$ while for $x = 0.2$ the crystal structure transformed to an ideal cubic structure (Nandan and Kumar, 2017). Generally, BaTiO_3 exhibits cubic structure at around 130°C , but in our case due to the strontium doping, we were able to achieve cubic structure at room temperature. This raised our interest to analyze the powder X-ray diffraction (XRD) data and herein we are reporting the powder XRD pattern for BSTO samples.

II. EXPERIMENTAL

A. Synthesis

Polycrystalline samples of $\text{Ba}_{0.8}\text{Sr}_{0.2}\text{Ti}_{0.6}\text{Zr}_{0.3}\text{Mn}_{0.1}\text{O}_3$ (BSTO) were prepared by a standard solid-state reaction method. Initially, precursors barium carbonate, strontium carbonate, titanium dioxide, zirconium oxide, and manganese oxides were weighed in stoichiometric ratios and mixed by a ball milling process. The homogeneous mixture was calcined up to 1550°C in air atmosphere with intermediate grindings. The experimental procedures are detailed in our previous report (Nandan and Kumar, 2017).

B. Data collection

Powder XRD data of the samples were measured using a Bruker D8 Advance (Germany) diffractometer. The sintered powders were ground and loaded in a zero background (911) Si single-crystal wafer holder. The instrument was operated in Bragg-Brentano geometry with fixed slits. The diffraction data for the sample was recorded using Cu $K\text{-}\alpha\text{-}1$ ($\lambda = 1.54060 \text{ \AA}$), $K\text{-}\alpha\text{-}2$ ($\lambda = 1.54439 \text{ \AA}$), and $K\text{-}\beta$ ($\lambda = 1.39222 \text{ \AA}$) radiation as the source which is operated at a

^{a)} Author to whom correspondence should be addressed. Electronic mail: nandan88.kr@gmail.com

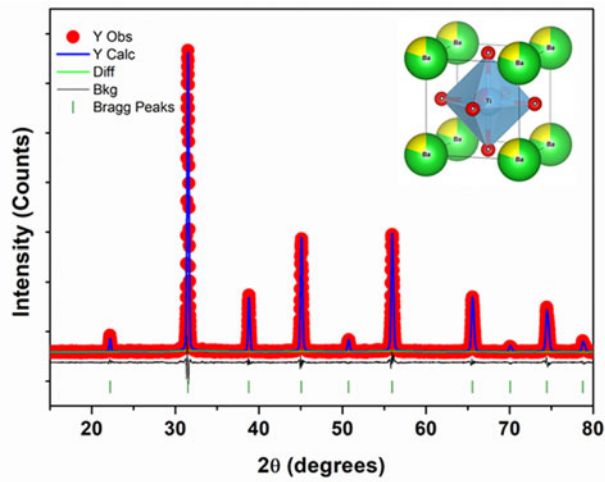


Figure 1. Rietveld refinement of powder XRD data of BSTO polycrystalline sample. The inset shows the BSTO crystal structure.

TABLE I. Fractional coordinates for BSTO samples.

Atoms	<i>x</i>	<i>y</i>	<i>z</i>	Occ	<i>U</i> _{iso}
Ba	0	0	0	0.8	0.0133 (20)
Sr	0	0	0	0.2	0.0133 (20)
Ti	0.5	0.5	0.5	0.6	0.027 (3)
Zr	0.5	0.5	0.5	0.3	0.027 (3)
Mn	0.5	0.5	0.5	0.1	0.027 (3)
O	0	0.5	0.5	1	0.103 (8)

TABLE II. Crystal data from GSAS program and Powder X software.

Crystal data from GSAS Program	Crystal data from Powder X software
Lattice parameters: <i>a</i> = <i>b</i> = <i>c</i> = 4.0253 (30) Å <i>α</i> = <i>β</i> = <i>γ</i> = 90° Volume = 65.22 (15) Å ³ <i>Z</i> = 3 Space group: <i>Pm</i> -3 <i>m</i> Crystal structure: Cubic <i>χ</i> ² = 1.873 <i>R</i> _{wp} = 7.597	Lattice parameters: <i>a</i> = <i>b</i> = <i>c</i> = 4.0321 (11) Å <i>α</i> = <i>β</i> = <i>γ</i> = 90° Volume = 65.55 Å ³ Space group: <i>Pm</i> -3 <i>m</i> Crystal structure: Cubic

voltage of 40 kV and a current of 30 mA with a goniometer radius of 217.5 mm. The data were recorded at a 2θ range from 10° to 80° with a step size of 0.015°.

TABLE III. Powder diffraction data of BSTO polycrystalline material.

S. No	2θ _{exp}	2θ _{cal}	2θ _{diff}	<i>d</i> _{exp}	<i>d</i> _{calc}	Intensity (exp)	<i>h</i>	<i>k</i>	<i>l</i>
1	22.146	22.161	-0.015	4.01077	4.02600	44	1	0	0
2	31.470	31.480	-0.01	2.84043	2.84681	1000	1	1	0
3	38.767	38.757	0.01	2.32093	2.32441	176	1	1	1
4	45.047	44.997	0.05	2.01088	2.013	372	2	0	0
5	50.701	50.660	0.041	1.79911	1.80048	38	2	1	0
6	55.926	55.895	0.031	1.64278	1.64361	433	2	1	1
7	65.535	65.526	0.009	1.42324	1.42341	205	2	2	0
8	70.049	70.058	-0.009	1.34215	1.342	19	2	2	1
9	74.451	74.464	-0.013	1.27332	1.27313	165	3	1	0
10	78.754	78.777	-0.023	1.21417	1.21388	41	3	1	1

TABLE IV. Selected bond lengths for BSTO samples.

Metal-oxygen	Bond length (Å)
Ti-O	2.01265
Zr-O	2.01265
Mn-O	2.01265
Ba-O	2.84632
Sr-O	2.84632

III. RESULTS

The refined powder XRD pattern for the BSTO samples is shown in Figure 1. Rietveld refinement for the diffraction data were carried by using GSAS-II program (Toby and Von Dreele, 2013). The initial structural parameters for refinement were taken from previous reports (Kim et al., 2004). The background was modeled using a Chebyshev polynomial. The fixed positional and isotropic displacement parameters were constrained for Ba and Sr to be the same and Ti, Zr, and Mn to be the same. Site occupancies were set and held fixed to the values determined by weights of the various starting materials mixed together and calcined given that no impurity phases evolved, even when sintered at higher temperatures. The powder data fitted well for *Pm*-3*m* space group and the fractional coordinates are shown in Table I. The results of the refinement (lattice parameter and *R* factors) are shown in Table II. The crystal structure of BSTO has been elucidated by Vesta software and shown as the inset in Figure 1 (Momma and Izumi, 2013). The experimental data were also indexed by Powder X software (Dong, 1999) and the results of the refined parameters are shown in Tables II and III. K-alpha-2 stripping has been done before peak indexing in Powder X software. The various metal-oxygen bond lengths from the refined data are given in Table IV.

IV. CONCLUSION

Polycrystalline samples of BSTO are prepared by a conventional solid-state reaction. Powder XRD patterns for the prepared sample confirmed the single-phase formation of the compound without any impurities. The prepared sample crystallized in a cubic structure (*Pm*-3*m* space group) with lattice parameters *a* = *b* = *c* = 4.0253 Å, *α* = *β* = *γ* = 90°. Rietveld refinement for the XRD pattern was done by GSAS program and the peak indexing was carried out by Powder X software.

V. DEPOSITED DATA

The Crystallographic Information Framework (CIF) file was deposited with the ICDD. The data can be requested at pdj@icdd.com.

REFERENCES

- Das, S. K., P. P. Rout, S. K. Pradhan, and B. K. Roul. 2012. "Effect of Equiproportional Substitution of Zn and Mn in BaTiO₃ Ceramic—An Index to Multiferroic Applications." *Journal of Advanced Ceramics* 1 (3): 241–8.
- Dong, C. 1999. "PowderX: Windows-95-Based Program for Powder X-Ray Diffraction Data Processing." *Journal of Applied Crystallography* 32: 4.
- Kim, Y. I., J. K. Jung, and K. S. Ryu. 2004. "Structural Study of Nano BaTiO₃ Powder by Rietveld Refinement." *Materials Research Bulletin* 39 (7–8): 1045–53.
- Levin, I., E. Cockayne, V. Krayzman, J. C. Woicik, S. Lee, and C. A. Randall. 2011. "Local Structure of Ba (Ti,Zr)O₃ Perovskite-like Solid Solutions and Its Relation to the Band-Gap Behavior." *Physical Review B* 83 (9): 094122.
- Momma, K., and F. Izumi. 2013. "VESTA 3 for Three-Dimensional Visualization of Crystal, Volumetric and Morphology Data." *Journal of Applied Crystallography* 44: 1272–6.
- Nandan, K. R., and A. R. Kumar. 2017. "Effect of Sr-Doping on Structure and Electrical Properties of (Ba_{1-x}Sr_xTi_{0.6}Zr_{0.3}Mn_{0.1}O₃)_{x=0.1} and 0.2 Synthesized by Solid State Reaction." *Journal of Materials Science: Materials in Electronics* 28 (10): 7221–30.
- Sindhu, M., N. Ahlawat, S. Sanghi, R. Kumari, and A. Agarwal. 2013. "Crystal Structure Refinement and Investigation of Electrically Heterogeneous Microstructure of Single Phased Sr Substituted BaTiO₃ Ceramics." *Journal of Alloys and Compounds* 575: 109–14.
- Toby, B. H., and R. B. Von Dreele. 2013. "GSAS-II: The Genesis of a Modern Open-Source All Purpose Crystallography Software Package." *Journal of Applied Crystallography* 46 (2): 544–9.
- Wang, J., G. Rong, T. Wang, and H. Yao. 2014. "Impact of Sr on the Performance of BaTi_{0.9}Zr_{0.1}O₃–BaTiO₃ Dielectric Powders." *Modern Physics Letters B* 28 (14): 1450114.
- Xue, D., Y. Zhou, H. Bao, J. Gao, C. Zhou, and X. Ren. 2011. "Large Piezoelectric Effect in Pb-free Ba(Ti,Sn)O_{3-x}(Ba,Ca)TiO₃ Ceramics." *Applied Physics Letters* 99 (12): 122901.
- Yu, Y., H. Zou, Q. F. Cao, X. S. Wang, Y. X. Li, and X. Yao. 2015. "Phase Transitions and Relaxation Behaviors in Barium Strontium Titanate Ceramics Determined by Dynamic Mechanical and Dielectric Analysis." *Ferroelectrics* 487 (1): 77–85.
- Zhou, L., P. M. Vilarinho, and J. L. Baptista. 1999. "Dependence of the Structural and Dielectric Properties of Ba_{1-x}Sr_xTiO₃ Ceramic Solid Solutions on Raw Material Processing." *Journal of the European Ceramic Society* 19 (11): 2015–20.